

Relaxation of ^{121}Sb NQR in Antimony Trichloride due to Raman Process

Noriaki Okubo and Mutsuo Igarashi^a

Institute of Physics, University of Tsukuba, Tsukuba, 305-8571 Japan

^a Department of Applied Physics, Gunma College of Technology, Maebashi, 371-8530 Japan

Reprint requests to Dr. N. O.; Fax: +81-298-53-6618; E-mail: nrkokubo@sakura.cc.tsukuba.ac.jp

Z. Naturforsch. **56a**, 777–784 (2001); received August 21, 2001

The spin-lattice relaxation times of ^{121}Sb nuclear quadrupole resonance in SbCl_3 have been measured from 4.2 K to the m. p., 346 K. The result is analyzed with a theory of the Raman process based on covalency and discussed in comparison with the previous result for ^{35}Cl nuclei.

Key words: SbCl_3 ; ^{121}Sb -NQR; Relaxation Times; Raman Process; Covalency.

1. Introduction

In the preceding papers [1–5] we have shown that the relaxation of NMR and NQR in several non-metallic compounds can be accounted for by a theory [6] of the Raman process based on covalency. In the case of SbCl_3 we reported that only on the chlorine NQR [2]. For this compound we also reported that a relaxation mechanism due to a certain kind of molecular motions works at high temperature. Now, two problems are left: The one is whether the relaxation of antimony nuclei can also be accounted for by the theory and whether the results are consistent with those for the chlorine nuclei. The other is whether the contribution of the molecular motions is also observed for the relaxation of antimony nuclei. However, there are several difficulties in applying the theory to antimony nuclei. In the next section the method of the measurement of the relaxation times of ^{121}Sb nuclei in SbCl_3 is described, and in the following section the results are presented. In Sect. 4, the expressions for the transition probabilities of the antimony nuclei are presented in a rather general form and the problems are discussed together with the difficulties. The conclusion is given in Section 5.

2. Experimental Procedure

As shown in Fig. 1, the energy diagram of ^{121}Sb nuclei (spin 5/2) consists of three levels E_m ($m = \pm 1/2, \pm 3/2, \pm 5/2$), and three transitions ν_i ($i = 1, 2, 3$) can be observed owing to a finite value of the asymmetry pa-

rameter η . Irrespective of the responsible interaction, the relaxation in a three-level system is governed by two relaxation times, T_{1+} and T_{1-} , and they are expressed with the transition probabilities W_α ($\alpha = a, b, c$) defined in Fig. 1 as follows:

$$T_{1\pm}^{-1} = W_a + W_b + W_c \pm \frac{1}{\sqrt{2}} \sqrt{(W_b - W_c)^2 + (W_c - W_a)^2 + (W_a - W_b)^2}, \quad (1)$$

where the upper and lower signs of the suffix of $T_{1\pm}^{-1}$ correspond to those on the right hand side, respectively. The recovery of the signal intensity $S_i(t)$ ($i = 1, 2, 3$) of the ν_i -line following application of a pulse at time $t = 0$

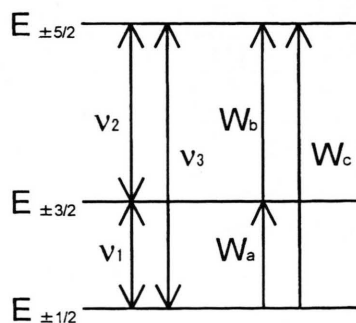


Fig. 1. Energy levels E_m ($m = \pm 1/2, \pm 3/2, \pm 5/2$), resonance frequencies ν_i ($i = 1, 2, 3$), and upward transition probabilities W_α ($\alpha = a, b, c$) for a three-level system. The corresponding downward transition probabilities are written as $W_\alpha(1 + \Delta_i)$ ($i = 1, 2, 3$). Energy levels are specified by the magnetic quantum number m of the eigen states for $\eta = 0$.

0932-0784 / 01 / 1100-0777 \$ 06.00 © Verlag der Zeitschrift für Naturforschung, Tübingen · www.znaturforsch.com



Dieses Werk wurde im Jahr 2013 vom Verlag Zeitschrift für Naturforschung in Zusammenarbeit mit der Max-Planck-Gesellschaft zur Förderung der Wissenschaften e.V. digitalisiert und unter folgender Lizenz veröffentlicht: Creative Commons Namensnennung-Keine Bearbeitung 3.0 Deutschland Lizenz.

Zum 01.01.2015 ist eine Anpassung der Lizenzbedingungen (Entfall der Creative Commons Lizenzbedingung „Keine Bearbeitung“) beabsichtigt, um eine Nachnutzung auch im Rahmen zukünftiger wissenschaftlicher Nutzungsformen zu ermöglichen.

This work has been digitalized and published in 2013 by Verlag Zeitschrift für Naturforschung in cooperation with the Max Planck Society for the Advancement of Science under a Creative Commons Attribution-NoDerivs 3.0 Germany License.

On 01.01.2015 it is planned to change the License Conditions (the removal of the Creative Commons License condition “no derivative works”). This is to allow reuse in the area of future scientific usage.

is represented as

$$\frac{S_i(\infty) - S_i(t)}{S_i(\infty)} = a_{i+} \exp\left(-\frac{t}{T_{1+}}\right) + a_{i-} \exp\left(-\frac{t}{T_{1-}}\right). \quad (2)$$

When the effect of applying a $\pi/2$ pulse on the ν_i -line is regarded as only equalizing the populations of the corresponding two levels, the coefficients for the ν_1 -line following the saturation of the ν_1 -line are written as

$$a_{1+} = \frac{-1/T_{1-} + (1/2 + \nu_2/\nu_1)(W_b - W_c)}{1/T_{1+} - 1/T_{1-}} \quad (3)$$

with

$$a_{1+} + a_{1-} = 1. \quad (4)$$

The derivation of (3) is given in Appendix A. The coefficients for the recovery of the ν_2 -line under the same condition are written as

$$a_{2+} = \frac{\nu_1/2\nu_2 T_{1-} - (1 + \nu_1/2\nu_2)(2W_b + W_c)}{1/T_{1+} - 1/T_{1-}} \quad (5)$$

with

$$a_{2+} + a_{2-} = -\frac{\nu_1}{2\nu_2}. \quad (6)$$

Similarly, when the effect of applying a π pulse on the ν_i -line is regarded as reversing the population of the corresponding levels, the coefficients for the ν_1 -line following the reversal of the ν_1 -line is given by

$$a_{1+} = \frac{-2/T_{1-} + 2W_a + (1 + \nu_2/\nu_1)W_b + (\nu_2/\nu_1)W_c}{1/T_{1+} - 1/T_{1-}} \quad (7)$$

with

$$a_{1+} + a_{1-} = 2. \quad (8)$$

The coefficients for the recovery of the ν_2 -line under this condition are determined as

$$a_{2+} = \frac{\nu_1/\nu_2 T_{1-} - (\nu_1/\nu_2)W_a - 2(1 + \nu_1/\nu_2)W_b - W_c}{1/T_{1+} - 1/T_{1-}} \quad (9)$$

with

$$a_{2+} + a_{2-} = -\frac{\nu_1}{\nu_2}. \quad (10)$$

The coefficients for the recovery curve of any line following the saturation or the reversal of any line are

determined in such a way. The transition probabilities W_α can be determined from the experiment of the saturation recovery on only one of the resonance lines, for example, through (1) and (3) from the values of T_{1+} , T_{1-} and a_{1+} . However, to determine them uniquely, another experiment is required. Since it is not easy to deal with two frequencies at the same time, in the present study the recovery of the ν_1 -line following the ν_1 -line saturation was examined, and the extra solutions were removed by the examination of the recovery of the ν_1 -line following the reversal of the ν_1 -line.

The energy diagram for ^{123}Sb nuclei (spin 7/2) consists of four levels, and the relaxation is governed by three time constants. Also, for a system with more than two relaxation times they can, in principle, be determined separately either by the usual method that the contribution appearing as the decay tail is subtracted from the whole recovery curve one after another on a log plot of $[S(\infty) - S(t)]/S(\infty)$, or by a least-squares-fitting with a computer. However, the requirements on the signal-to-noise ratio and the stability rapidly become hard as the number of the involved relaxation times increases. In the present study only ^{121}Sb nuclei were treated.

The sample and the apparatus were the same as in [2]. A signal averaging was employed with repeating times longer than several times of T_1 at given temperatures. A least-squares-fitting of (2) to the recovery curve was performed to obtain T_{1+} , T_{1-} and a_{1+} .

In observing the recovery at a given temperature, the rf pulses were applied with the exact resonance frequency. On the other hand, in analyzing the data using (1), (3), and (7) such an accuracy of the frequency is not required and the values reported in [7] were used for ν_2 .

3. Results

The temperature dependence of the frequency ν_1 of the ^{121}Sb NQR measured by us can be represented by the polynomial

$$\nu_1(T) = c_0 + c_1 T + c_2 T^2 + c_3 T^3 \quad (11)$$

with the values of the coefficients given in Table 1. The result agrees with those reported over various temperature ranges by several groups [7].

Figure 2 shows the temperature dependence of two relaxation times T_{1+} and T_{1-} . For the cases where the measurement was done more than one times at the same temperature, the averaged values are shown. Roughly

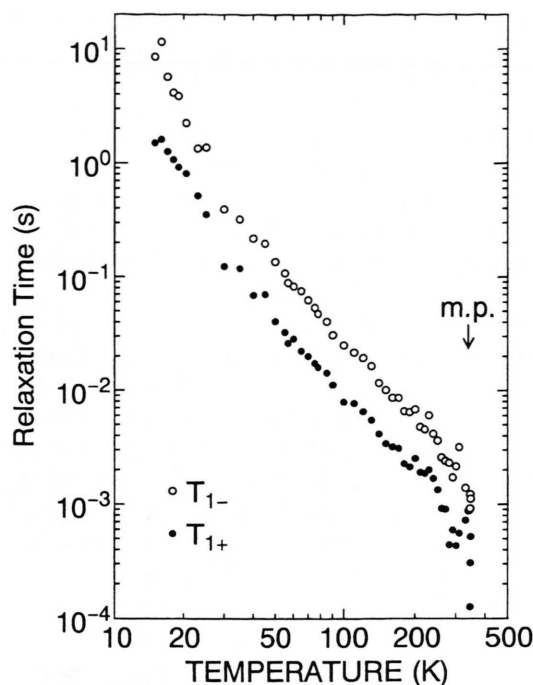


Fig. 2. Temperature dependence of the relaxation times T_{1+} and T_{1-} . Note that the ordinate and the abscissa are drawn in a different scale.

Table 1. Coefficients of $\nu_1(T)$ according to (11), determined by a least-squares-fitting for 57 data from 4.2 to 346 K, and standard deviation σ .

Coefficients	Values	
c_0	59.8805	(MHz)
c_1	-2.79493×10^4	(MHz/K)
c_2	-2.42091×10^{-5}	(MHz/K ²)
c_3	-1.81582×10^{-8}	(MHz/K ³)
σ	0.0064842	(MHz)

estimated values of T_{1+} and T_{1-} at 4.2 K were 34 and 330 s, respectively. As in the case of ^{35}Cl nuclei [2] the slopes of $T_1(T)$ continued to increase down to such a low temperature. This implies that T_1 does not suffer the effect of impurities. The slope becomes progressively gentler with increasing temperature and remains about -2 up to about 250 K, but it becomes again progressively steeper up to melting point (346 K), suggesting the existence of molecular motions at high temperatures. Correspondingly the signal intensity, which decreased nearly in proportion to T^{-1} up to 250 K, decreased more rapidly above 250 K. The value of the coefficient a_{1+}

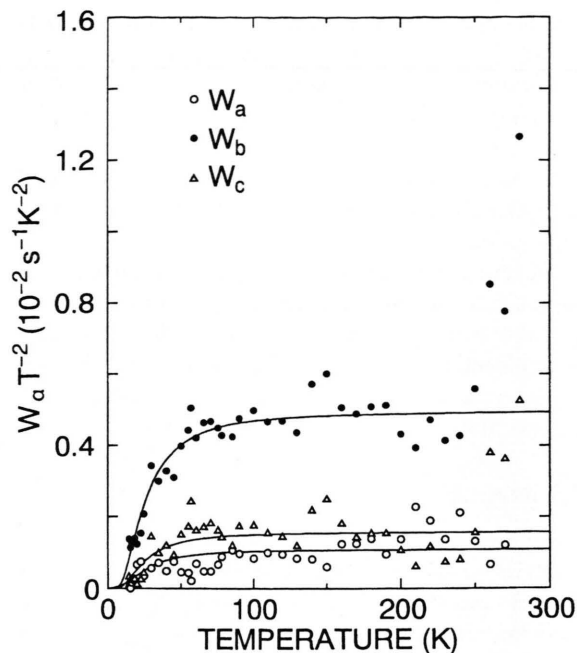


Fig. 3. Temperature dependence of $W_\alpha T^{-2}$ ($\alpha = a, b, c$). The solid curves are drawn for the values in Table 4. Only the data points up to 280 K are shown.

decreased from about 0.9 at low temperatures to about 0.5 at high temperatures.

The values of T_{1+} , T_{1-} and a_{1+} were converted into W_a , W_b , and W_c by the use of (1) and (3). The extra solution could be removed definitely by observing the inversion recovery at 77 K. The observation at one temperature is sufficient for this purpose, because if the exchange of the solutions happened at any temperature, the temperatures dependence of W_α would exhibit a discontinuity in spite of the continuity of the T_1 's. Figure 3 shows the temperature dependence of a thus determined set of W_α 's, where only the data points up to 280 K are plotted because above it the scattering rapidly becomes large owing to the lowering of the signal intensity.

The values of T_2 and T_2^* obtained for the ν_1 -line were 860 and 19.5 μs , respectively, at 77 K.

4. Analysis and Discussion

4.1. Relaxation Mechanism

In the case of chlorine nuclei, the magnetic and the quadrupolar relaxation mechanisms could be discrimi-

nated simply by comparing the isotopic ratio of the observed T_1^{-1} with the squared ratios of the magnetic dipole moments and the quadrupole moments. This method cannot be applied in the case of antimony nuclei, because the expressions for T_1 differ between ^{121}Sb and ^{123}Sb nuclei, and moreover it is difficult to separately determine three T_1 's for ^{123}Sb nuclei with sufficient accuracy.

As seen in Fig. 2, the temperature dependence of T_1 approaches a T^{-2} dependence at high temperatures except above 250 K. This suggests that the Raman process is dominant, as in the case of ^{35}Cl nuclei. In the following the relaxation is analyzed by assuming the Raman process alone.

4.2. Raman Process

We have shown that a theory of the Raman process based on covalency [6] can account for the relaxation in several compounds [1–5]. The theory assumes some conditions. Parts of them have been released by our extension. First, the condition of inversion symmetry of the molecule was made ineffective by including cross-terms in the calculation of $L_\nu(ka)$, as shown later. Second, the condition of equivalence of the ions was loosened to the condition of equi-distance by using different $N_{\mu\nu}$ and D_ν values for different bond pairs as shown below. For the quadrupolar relaxation, the transition probabilities from the level m to level $m + \mu$ ($\mu = 1, 2$), $P(m, m + \mu)$, are written as [8]

$$P(m, m+1) = \frac{(2m+1)^2(I-m)(I+m+1)}{2I(2I-1)^2} W_1, \\ P(m, m+2) = \frac{(I-m-1)(I+m+2)(I-m)(I+m+1)}{2I(2I-1)^2} W_2. \quad (12)$$

If in an AB_x type molecule the condition of axial symmetry for the EFG about the bond A-B is satisfied, W_μ ($\mu = 1, 2$) for nuclei A is expressed as

$$W_1 = \frac{10A'^2c^3}{\pi^3a^7d^2v^3} T^{*2} \cdot \sum_{\{n, n'\}} \sum_{\nu=1}^3 N_{1\nu}(\phi_{nn'}) D_\nu(T^*, \phi_{nn'}), \\ W_2 = \frac{40A'^2c^3}{\pi^3a^7d^2v^3} T^{*2} \cdot \sum_{\{n, n'\}} \sum_{\nu=1}^3 N_{2\nu}(\phi_{nn'}) D_\nu(T^*, \phi_{nn'}), \quad (13)$$

where

$$A' = \frac{3}{100} e^2 Q \left\langle \frac{1}{r^3} \right\rangle_A \quad (14)$$

for spin $I = 5/2$. $\langle r^{-3} \rangle_A$ means the expectation value with respect to the valence p electron of an A atom. In (13) the first summation is made over the combination of bonds n and n' between A and B atoms. To avoid the unduly increase of the suffix ν with increase of the number of bonds, $N_{\mu\nu}$ and D_ν are regarded as functions of the angle $\phi_{nn'}$ between bonds n and n' . $N_{\mu\nu}$ is also a function of λ , as shown in Appendix B, where λ is a measure of covalency of the bond [6]. a denotes the bond length, d the density, T^* the temperature reduced by the Debye temperature θ_D . c is defined as $c = k_D a$ with the maximum wave number $k_D = (6\pi^2 N/V)^{1/3}$, N being the number of atoms in the unit cell of volume V . $v = \nu k_B \theta_D / \hbar k_D$ is the sound velocity. D_ν is defined as

$$D_\nu(T^*, \phi_{nn'}) = T^* \int_0^{1/T^*} \frac{x^2 e^x}{(e^x - 1)^2} L_\nu(cT^* x, \phi_{nn'}) dx \\ (\nu = 1 \text{ to } 3) \quad (15)$$

with

$$L_1(ka, \phi_{nn'}) = \left[\frac{1}{2} f(ka \sqrt{2(1 - \cos \phi_{nn'})}) - \frac{1}{2} f(2ka \sqrt{2(1 + \cos \phi_{nn'})}) \right]^2, \\ L_2(ka, \phi_{nn'}) = \left[1 - 2f(ka) + \frac{1}{2} f(ka \sqrt{2(1 - \cos \phi_{nn'})}) + \frac{1}{2} f(2ka \sqrt{2(1 + \cos \phi_{nn'})}) \right]^2, \\ L_3(ka, \phi_{nn'}) = 2 \left[\frac{1}{2} f(ka \sqrt{2(1 - \cos \phi_{nn'})}) - \frac{1}{2} f(2ka \sqrt{2(1 + \cos \phi_{nn'})}) \right]^2 \\ \times \left[1 - 2f(ka) + \frac{1}{2} f(ka \sqrt{2(1 - \cos \phi_{nn'})}) + \frac{1}{2} f(2ka \sqrt{2(1 + \cos \phi_{nn'})}) \right], \quad (16)$$

where $f(y) = \text{siny}/y$.

4.3. Transition Probabilities

When η is small and consequently the mixing among the states can be neglected, W_a is given by summing up $P(1/2 \rightarrow 3/2)$, $P(-1/2 \rightarrow -3/2)$, $P(-1/2 \rightarrow 3/2)$, and

Table 2. Crystal [9] and ^{121}Sb NQR [10] data of SbCl_3 .

N	V (\AA^3)	a (\AA)	ϕ ($^\circ$)	d (g/cm^3)	e^2Qq_{mol} (MHz)	η
16	482.3	2.340 (Sb-Cl_1)	95.70 ($\text{Cl}_1\text{-Sb-Cl}_{2,3}$)	3.141	383.762 ^a	0.187035 ^a
		2.368 ($\text{Sb-Cl}_{2,3}$)	90.98 ($\text{Cl}_2\text{-Sb-Cl}_3$)			

^a at 78.6 K.

$P(1/2 \rightarrow -3/2)$, while W_b is given as a sum of $P(3/2 \rightarrow 5/2)$ and $P(-3/2 \rightarrow -5/2)$, and W_c is given as a sum of $P(1/2 \rightarrow 5/2)$ and $P(-1/2 \rightarrow -5/2)$. The use of (12) for these $P(m, m')$'s yields

$$\begin{aligned} W_a &= \frac{4}{5} W_1 + \frac{9}{5} W_2, \\ W_b &= 2W_1, \\ W_c &= W_2. \end{aligned} \quad (17)$$

Then, we get the following forms convenient for fitting:

$$\begin{aligned} W_\alpha T^{-2} &= (\tau_\alpha \theta_D^2)^{-1} \\ &\cdot \left[\varepsilon_\alpha(\phi_{11}) \sum_{v=1}^3 D_v(T^*, \phi_{11}) + \varepsilon_\alpha(\phi_{12}) \right. \\ &\cdot \sum_{v=1}^3 D_v(T^*, \phi_{12}) + \varepsilon_\alpha(\phi_{23}) \sum_{v=1}^3 D_v(T^*, \phi_{23}) \end{aligned} \quad (18)$$

$(\alpha = a, b, c),$

where

$$\begin{aligned} \frac{1}{\tau_a} &= \frac{9e^4 Q^2 \langle r^{-3} \rangle_{\text{Sb}}^2 c^3}{1250 \pi^3 a^7 d^2 v^3} N_{11}(\phi_{11}), \\ \frac{1}{\tau_b} &= \frac{9e^4 Q^2 \langle r^{-3} \rangle_{\text{Sb}}^2 c^3}{500 \pi^3 a^7 d^2 v^3} N_{11}(\phi_{11}), \\ \frac{1}{\tau_c} &= \frac{9e^4 Q^2 \langle r^{-3} \rangle_{\text{Sb}}^2 c^3}{250 \pi^3 a^7 d^2 v^3} N_{21}(\phi_{11}), \end{aligned} \quad (19)$$

and

$$\begin{aligned} \varepsilon_a(\phi_{nn'}) &= \frac{N_{11}(\phi_{nn'}) + 9N_{21}(\phi_{nn'})}{N_{11}(\phi_{11})}, \\ \varepsilon_b(\phi_{nn'}) &= \frac{N_{11}(\phi_{nn'})}{N_{11}(\phi_{11})}, \\ \varepsilon_c(\phi_{nn'}) &= \frac{N_{21}(\phi_{nn'})}{N_{21}(\phi_{11})}. \end{aligned} \quad (20)$$

Though η for the Sb nuclei of SbCl_3 is not so small as shown in Table 2, in the following it is assumed to vanish for brevity. Consequently, agreement between

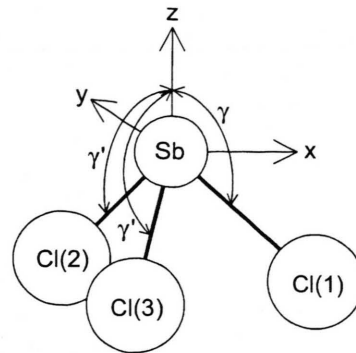


Fig. 4. The principal axis system of the EFG at Sb nuclei. The x -axis is so taken that the xz plane includes the $\text{Cl}(1)$ atom and bisects the angle $\text{Cl}(2)\text{-Sb-Cl}(3)$. Only the direction cosines with respect to the z -axis are shown by the arched arrows.

Table 3. Values of $N_{\mu\nu}(\phi_{nn'})$ ($\nu = 1, 2, 3$). The weighted average 2.359 \AA was used for a . $\phi_{12}(=\phi_{13})$ is assumed to be equal to ϕ_{23} , and the weighted average 94.13° was used for them.

μ	$\phi_{nn'}$	$N_{\mu\nu}$ in unit of λ^2
1	$\phi_{11} = \phi_{22} = \phi_{33}$	1634.38
	$\phi_{12} = \phi_{13}$	608.657
	ϕ_{23}	304.329
2	$\phi_{11} = \phi_{22} = \phi_{33}$	313.537
	$\phi_{12} = \phi_{13}$	100.725
	ϕ_{23}	50.353

the experiment and the theory is not pursued with high accuracy.

4.4. Debye Temperature

In the crystal, one Cl atom of SbCl_3 occupies site I ($\text{Cl}(1)$) and two occupy site II ($\text{Cl}(2)$ and $\text{Cl}(3)$). $N_{\mu\nu}$ is calculated for the principal axis system of the EFG at Sb nuclei, as shown in Figure 4. The direction cosines of the $\text{Sb-Cl}(1)$ bond is denoted by $(\alpha, 0, \gamma)$, and those of $\text{Sb-Cl}(2)$ and $\text{Sb-Cl}(3)$ bonds by $(\alpha', \beta', \gamma')$ and $(\alpha', -\beta', \gamma')$, respectively. The following relation is assumed for the measure of covalency λ as in [1-5]:

$$\lambda \propto \exp\left(-\frac{r}{Q}\right), \quad (21)$$

where Q is the repulsive range parameter and r the atomic distance. Using a value $a = 2.359 \text{ \AA}$ as the weighted average of bond lengths together with a value $Q = 0.345 \text{ \AA}$ [6] we can express $N_{\mu\nu}$ as a function of γ and γ' only, as shown in Appendix B. Then we obtain the values listed in Table 3 for $N_{\mu\nu}$. The values of $\varepsilon(\phi_{nn'})$

Table 4. The results of the fitting of $W_\alpha T^{-2}$ ($\alpha = a, b, c$).

	W_a	W_b	W_c
$\theta_D(\text{K})$	(98.2)	98.2	(98.2)
$\tau_\alpha(\text{s})$	0.2457	0.0199	0.0621

are obtained from the values of $N_{\mu\nu}(\phi_{nn'})$ through (20). $D_\nu(\phi_{nn'})$ was calculated numerically for various T^* . Then (18) can be fitted to each $W_\alpha T^{-2}$ in Fig. 3 by scaling W_α and T respectively with τ_α^{-1} and θ_D as fitting parameters. The results are shown in Table 4. In the fitting of W_a and W_c , θ_D was fixed at the value obtained for W_b , 98.2 K, because the scattering is large and reasonable values were not obtained for them. Data up to 250 K were employed because above this temperature contributions from molecular motions seems to be significant. The value of θ_D obtained from the ^{35}Cl relaxation was 141.2 K. On the other hand, from the X-ray analysis values from 106.1 to 121.2 K are obtained for Sb atoms [2].

4.5. Covalency

In the case of halogen nuclei the coupling constants for the free atoms are reported, so that the values of λ could be determined from the values of τ and could be compared with the ratio of the coupling constant of the molecule to that of the free atom, $f = e^2 Q q_{\text{mol}} / e^2 Q q_{\text{at}}$, [1–3]. In the case of antimony nuclei the coupling constant for the free atom is not reported. Moreover, λ should not be compared directly with f . However, since $\langle r^{-3} \rangle_{\text{Sb}} = (5/4) q_{\text{at}}$ for a p electron, $e^2 Q \langle r^{-3} \rangle_{\text{Sb}}$ can be replaced by $(5/4) e^2 Q q_{\text{mol}} / f$. Then we can use the value in Table 2 for $e^2 Q q_{\text{mol}}$ and get the following expression for τ_α from (19):

$$\tau_\alpha = \tau_\alpha^0 (f/\lambda)^2, \quad (22)$$

where $\tau_a^0 = 4.39 \times 10^{-4}$ s, $\tau_b^0 = 1.75 \times 10^{-4}$ s, and $\tau_c^0 = 4.57 \times 10^{-4}$ s. Equating these τ_α with the values in Table 4 we get for λ/f the values of 0.0423, 0.0937, and 0.0858 from τ_a , τ_b , and τ_c , respectively. To determine the value of λ another relation between f and λ is required. If, for the brevity, C_3 symmetry is assumed for the molecule and the Townes-Dailey's theory is applied, f is represented as [11]

$$f = 2(1 - 2 \cot^2 \theta) + \frac{3 \cos^2 \theta - 1}{\sin^2 \theta} \lambda$$

$$= \frac{3 \cos \phi}{1 - \cos \phi} (\lambda - 2), \quad (23)$$

where θ denotes the angle each Sb–Cl makes with the C_3 axis and ϕ is the angle between Sb–Cl bonds. The expression of the first line is derived by considering the sp^3 hybridized orbitals, one of which accommodates two electrons of the lone pair and the remainder each accommodates λ electrons corresponding to the Sb–Cl bond. In going to the second line, the relation between θ and ϕ for this symmetry, $\sin^2 \theta = 2(1 - \cos \phi)/3$, is used. When a value of 94.13° is used for ϕ as the weighted average, values of 0.017, 0.037, and 0.034 are obtained for λ , corresponding to the above obtained values for λ/f . These are by one order of magnitude smaller than the values of 0.284 and 0.260 for λ obtained from the ^{35}Cl relaxation [2]. Though the value of λ depends on ϕ , the situation is not improved even by taking into account the ambiguity of ϕ . Though the value of λ depends on $\theta_D^{5/2}$, λ is still much smaller even if the value of 141.2 K obtained from the ^{35}Cl relaxation is used.

The discrepancy is not restricted in the absolute magnitude. The relative magnitudes of τ_α^{-1} expected from (19) are $\tau_a^{-1} : \tau_b^{-1} : \tau_c^{-1} = N_{11}(\phi_{11})/5 : N_{11}(\phi_{11})/2 : N_{21}(\phi_{11})$, which, according to Table 3, are 327:817:314, whereas the determined ones are 4.07:50.3:16.1 as calculated from Table 4. The third discrepancy lies in the ratio of T_{1+} and T_{1-} . Substitution of (17) into (1) yields

$$\frac{T_{1+}^{-1}}{T_{1-}^{-1}} = \frac{14(1+w) + \sqrt{76 - 88w + 61w^2}}{14(1+w) - \sqrt{76 - 88w + 61w^2}}, \quad (24)$$

where

$$w = \frac{W_2}{W_1} = \frac{4 \sum_{\{n, n'\}} \sum_\nu N_{2\nu}(\phi_{nn'}) D_\nu(T^*, \phi_{nn'})}{\sum_{\{n, n'\}} \sum_\nu N_{1\nu}(\phi_{nn'}) D_\nu(T^*, \phi_{nn'})}. \quad (25)$$

As w increases from 0, the ratio T_{1+}^{-1}/T_{1-}^{-1} decreases from 4.30 and takes a minimum 1.66 at $w = 1.1$ and approaches 3.52 at $w = \infty$. The numerical calculation for SbCl_3 shows that, except $T^* < 0.1$, w takes a nearly constant value 0.76, corresponding to $T_{1+}^{-1}/T_{1-}^{-1} = 1.74$, whereas the observed values are close to 3~4. The fourth discrepancy appears in a_{1+} given by (3), which is written as

$$a_{1+} = \frac{-9 - 16.5w + \sqrt{76 - 88w + 66w^2}}{2\sqrt{76 - 88w + 66w^2}}. \quad (26)$$

The right hand side is negative for all values of w , in contrast with the observed values $a_{1+} = 0.5 \sim 0.9$.

These discrepancies may be attributed to the fact that this compound does not satisfy the conditions

which are assumed in the theory of the Raman process based on covalency [6]. First, the theory assumes axial symmetry of the EFG around the bond, whereas in SbCl_3 , even if covalency is supposed in only one Sb–Cl bond together with pure ionicity in other bonds, the lone pair electrons destroy the axial symmetry about that bond. In fact, when Sb^{+3} ion forms covalent bonding with one Cl atom with λ electrons in the orbital directed toward the Cl atom together with the lone pair, and the z axis is taken along the Sb–Cl bond, η is expressed as

$$\eta = \frac{3(1 - \alpha^2) \sin^2 \theta}{(1 - \alpha^2)(2 - 3 \sin^2 \theta) + \lambda(1 - \beta^2)}, \quad (27)$$

where α and β denote the amounts of s -character of the lone pair orbital and the Sb–Cl bond orbital, respectively, and they are related with θ by $\alpha^2 = 2 \cot^2 \theta$ and $\beta^2 = (3 \sin^2 \theta - 2)/3 \sin^2 \theta$. When any value obtained for λ is used together with the value $\phi = 94.13^\circ$, $|\eta|$ becomes larger than unity, far from the axial symmetry. Second, the finite η causes the mixing of the states, and then $W_\alpha (\alpha = a, b, c)$ is not related with $W_i (i = 1, 2)$ by (17), and moreover W_0 is also required. The discrepancy about a_{1+} originates only from the neglect of the mixing. To meet the actual situation, the theory must be modified from the first stage and it is considerably laborious. In addition, the contribution from d electrons may have to be taken into consideration [10].

The expressions derived for W_1 and W_2 , (13), may be applied to NMR in SbCl_3 , for example, because the condition of axial symmetry is satisfied and in NMR the mixing is also negligible owing to the large Zeeman interaction. However, too small values of λ were also obtained for the bridging halogen nuclei in metal halides, [1, 3] and ^{27}Al nuclei in AlBr_3 , [4]. The present theory seems to give too large relaxation rates for multi-bond systems.

5. Conclusion

The spin lattice relaxation times of ^{121}Sb NQR in SbCl_3 have been measured between 4.2 K and the melting point. They were converted into transition probabilities, and up to this point the results are correct. When they are compared with the theory of the Raman process based on covalency, significant discrepancies were found in several respects. All these discrepancies are attributed mainly to the neglect of the destruction of axial

symmetry of the EFG about the bond by the lone pair. In addition, they originate partly from the neglect of mixing of the states among the levels and partly from the neglect of the contribution of d electrons. At high temperatures near the melting point a contribution of some molecular motions was observed as in the ^{35}Cl relaxation.

Appendix A Derivation of the Recovery Curve

In the following the high temperature approximation is used. When the population of the level $E_m (m = \pm 1/2, \pm 3/2, \pm 5/2)$ is denoted by $N_i (i = |m| + 1/2)$, the rate equations are written as

$$\begin{aligned} \frac{dN_3}{dt} &= -N_3[W_b(1 + \Delta_2) + W_c(1 + \Delta_3)] \\ &\quad + N_2W_b + N_1W_c, \\ \frac{dN_2}{dt} &= N_3W_b(1 + \Delta_2) - N_2[W_a(1 + \Delta_1) + W_b] \\ &\quad + N_1W_a, \\ \frac{dN_1}{dt} &= N_3W_c(1 + \Delta_3) + N_2W_a(1 + \Delta_1) \\ &\quad - N_1(W_c + W_a). \end{aligned}$$

The solutions are given by

$$N_i(t) = N_i(\infty) \left[1 - a_{i+} \exp\left(-\frac{t}{T_{1+}}\right) - a_{i-} \exp\left(-\frac{t}{T_{1-}}\right) \right],$$

where $N_i(\infty)$ are the values at thermal equilibrium and are written as

$$\begin{aligned} N_3(\infty) &= \frac{N}{3} \left(1 - \frac{1}{3} \Delta_1 - \frac{2}{3} \Delta_2 \right), \\ N_2(\infty) &= \frac{N}{3} \left(1 - \frac{1}{3} \Delta_1 + \frac{1}{3} \Delta_2 \right), \\ N_1(\infty) &= \frac{N}{3} \left(1 + \frac{2}{3} \Delta_1 + \frac{1}{3} \Delta_2 \right), \end{aligned}$$

where N denotes the total population and $\Delta_i = h\nu_i/k_B T$ ($i = 1, 2, 3$). When a $\pi/2$ pulse is applied to the ν_1 -transition at time $t = 0$, the initial condition is given by

$$\begin{aligned} N_3(0) &= N_3(\infty), \\ N_1(0) = N_2(0) &= \frac{1}{2} (N_1(\infty) + N_2(\infty)) \\ &= \frac{N}{3} \left(1 + \frac{1}{6} \Delta_1 + \frac{1}{3} \Delta_2 \right). \end{aligned}$$

These use of these conditions yields

$$\begin{aligned} a_{3+} + a_{3-} &= 0, \\ \frac{a_{3+}}{T_{1+}} + \frac{a_{3-}}{T_{1-}} &= \left(\frac{1}{2} \Delta_1 + \Delta_2 \right) (W_b + W_c), \\ a_{2+} + a_{2-} &= -\frac{1}{2} \Delta_1, \\ \frac{a_{2+}}{T_{1+}} + \frac{a_{2-}}{T_{1-}} &= -\left(\frac{1}{2} \Delta_1 + \Delta_2 \right) W_b, \\ a_{1+} + a_{1-} &= \frac{1}{2} \Delta_1, \\ \frac{a_{1+}}{T_{1+}} + \frac{a_{1-}}{T_{1-}} &= -\left(\frac{1}{2} \Delta_1 + \Delta_2 \right) W_c. \end{aligned}$$

These determine a_{i+} and a_{i-} . Since the signal intensity is proportional to the population difference between the corresponding levels, the coefficients a_{i+} and a_{i-} are determined as in (3) and (5) in the text. In the case of application of a π -pulse the initial conditions are replaced by

$$\begin{aligned} N_3(0) &= N_3(\infty), \\ N_2(0) &= N_1(\infty), \\ N_1(0) &= N_2(\infty). \end{aligned}$$

Appendix B Calculation of $N_{\mu\nu}$

$N_{\mu\nu}$ is given as a sum of the term $\sum_{pp'} w_{1n}^* w_{1n'}$ in (4.35) of [6] for the possible combinations of bonds n and n' . If, in calculating the sums for various $\phi_{nn'}$, the relations

$$\begin{aligned} \alpha^2 + \gamma^2 &= 1, \\ \alpha'^2 + \beta'^2 + \gamma'^2 &= 1, \\ \alpha\alpha' + \gamma\gamma' &= \cos\phi_{12} = \cos\phi_{13}, \\ \alpha'^2 - \beta'^2 + \gamma'^2 &= \cos\phi_{23} \end{aligned}$$

are used to eliminate α , α' , and β' , we obtain $N_{\mu\nu}(\phi_{nn'})$ as a function of λ and γ' and variables u and v defined as

$$\begin{aligned} u &= \frac{1}{2} \lambda' - \lambda, \\ v &= 4\lambda - \frac{5}{2} a\lambda' + \frac{1}{2} a^2 \lambda'', \end{aligned}$$

where λ' and λ'' are the first and second derivatives with respect to r .

- [1] N. Okubo, H. Sekiya, C. Ishikawa, and Y. Abe, Z. Naturforsch. **47a**, 713 (1992).
- [2] N. Okubo and Y. Abe, Z. Naturforsch. **49a**, 680 (1994).
- [3] N. Okubo, M. Igarashi, and R. Yoshizaki, Z. Naturforsch. **50a**, 737 (1995).
- [4] N. Okubo, M. Igarashi, and R. Yoshizaki, Z. Naturforsch. **51a**, 277 (1996), where the term $(1/15)(3\cos^2\phi - 1)v^2$ in the bracket of (7) should be multiplied by $\cos^2\phi$, and '(1994)' in [14] should read '1'.
- [5] N. Okubo and M. Igarashi, Phys. Stat. Sol. (b) **215**, 1109 (1999).
- [6] K. Yosida and T. Moriya, J. Phys. Soc. Japan **11**, 33 (1956).
- [7] See references in [2].
- [8] E. R. Andrew and D. P. Tunstall, Proc. Phys. Soc. **78**, 1 (1961).
- [9] A. Lipka, Acta Cryst. **B35**, 3020 (1979).
- [10] H. Chihara, N. Nakamura, and H. Okuma, J. Phys. Soc. Japan **24**, 306 (1968).
- [11] T. P. Das and E. L. Hahn, Nuclear Quadrupole Resonance Spectroscopy, Solid State Physics, F. Seitz and D. Turnbull (Academic Press, New York 1958) Supplement 1. In (7.52) of [10] the replacement of $(1 - I)$ by λ yields (23) in the text.